Triassic sauropodomorph eggshell might not be soft

Seung Choi[1,2*], Tzu-Ruei Yang[3,4], Miguel Moreno-Azanza[5–7], Shukang Zhang[2], Noe-Heon Kim[8]

[1]Department of Earth Sciences, Montana State University, Bozeman, MT, USA. [2]Institute of Vertebrate Paleontology and Paleoanthropology, Chinese Academy of Sciences, Beijing, China. [3]Department of Geology, National Museum of Natural Sciences, Taichung, Taiwan. [4]Department of Earth Sciences, National Cheng Kung University, Tainan, Taiwan. [5]Aragosaurus: Recursos Geológicos y Paleoambientes – IUCA, Universidad de Zaragoza, Zaragoza, Spain. [6]Geobiotec, Departamento de Ciências da Terra, Universidade Nova de Lisboa, Caparica, Portugal. [7]Espaço Nova Paleo, Museu da Lourinhã, Lourinhã, Portugal. [8]School of Earth and Environmental Sciences, Seoul National University, Seoul, South Korea.

*e-mail: seung0521@gmail.com

(1200/1200 words)

The fossil record of dinosaur eggs is highly biased; dissimilar to the relatively rich egg record for theropods and sauropodomorphs[1,2], ceratopsian eggs have remained unknown due to the absence of embryo-containing eggs. Recently, based on the well preserved *Protoceratops* (Ceratopsia) and *Mussaurus* (Sauropodomorpha) eggs, Norell et al.[3] suggested a new hypothesis: first dinosaur eggs were soft, and thus extremely dissimilar to rigid eggs of Cretaceous dinosaurs and rigid eggshells were independently acquired by theropods, sauropodomorphs, and ornithopods. While we acknowledge that this hypothesis is a practical working hypothesis and may be eventually true, the interpreted 'soft *Mussaurus* eggshell'[3] is doubtful and may undermine their conclusion and mislead the interpretations of other fossil eggshells. The 'soft *Mussaurus* eggshell' interpretation, therefore, requires a rigorous verification based on a solid understanding of the biomineralization of *Mussaurus* eggshell.

We have three concerns on the methodologies. First, the Raman spectrum of *Mussaurus* eggshell is indicative of rigid eggshell. The *Mussaurus* eggshell presents a diagnostic peak for calcite (~1080 cm^{-1}) in the Raman spectrum, which is, however, interpreted as exogeneous (abiogenic) calcite since the surrounding limestone presents an identical signal[3]. Besides, the authors report that their spectra were replicated at three different positions in the eggshell, indicative of widespread calcite throughout the eggshell. Admittedly, the authors might have targeted, in all cases, exogeneous calcite inside the eggshell, but point analysis has a limitation for this purpose because no one can assure that the selected Raman points are optimal sampling set of a ‘population’ (i.e. *Mussaurus* eggshell). In addition, it should be emphasized that even a biogenic rigid eggshell can be recrystallized and substituted by abiogenic calcite[4]. In this case, differentiating biogenic calcite from abiogenic calcite by using point analysis of Raman spectroscopy alone is very hard task. A more parsimonious scenario that should have been falsified is that the eggshell is completely composed of calcite (rigid eggshell). For instance, rigid eggshell fossils are mostly composed of dense calcite, but sedimentary calcite is patchily distributed at surrounding siliciclastic matrix[5] (e.g. Fig. 1a–c). If the calcite in the *Mussaurus* eggshell is abiogenic[3], the calcite distribution in the eggshell would be as patchier as the surrounding matrix and not be perfectly consistent with the outline of *Mussaurus* eggshell.

Diverse analytical techniques, especially those offering line or two-dimensional mapping analyses that reveal the calcite distribution[4–7], could potentially resolve the ‘soft eggshell’[3] issue because results from Raman spectroscopy point analysis alone (spectrum) needs cross-validation by an independent approach. For example, electron backscatter diffraction (EBSD) analysis is a technique informing on the origin of the calcite by revealing its distribution and crystallographic orientation in an eggshell. Specifically, if the calcite in *Mussaurus* eggshell is indeed abiogenic[3], then the crystal orientation would be irregularly arranged as observed in abiogenic calcite and recrystallized eggshell[4,7]. In contrast, if the calcite indeed came from *Mussaurus* and has been unaltered, then it would yield crystallographic configuration of archosaur eggshells[4,5,7]. Elemental mapping using electron probe micro-analyzer (EPMA) (e.g. Fig. 1b, c) or energy-dispersive X-ray spectroscopy (EDX) focused on Ca (as a proxy of calcite), or even Raman mapping aimed at calcite (~1080 cm^{-1})

(see an example of Raman mapping aimed at amorphous carbon (~1580 cm^{-1}); Fig. 1f) are also feasible approaches that enable independent test on our hypothesis of 'rigid *Mussaurus* eggshell'.

Secondly, Norell et al.[3] assigned 1349, 1379, 1565, 1607, and 1700 (cm^{-1}) Raman peaks to protein fossilized products (PFPs), which correspond to *N*-, *S*-, *O*-heterocyclic polymers. Norell et al.[3] further stated that carbonyl, *N*- and *O*-heterocycles are potent mineral-coordinating ligands and they represent markers for biomineralization (see also Wiemann et al.[8]). However, soot[9], amorphous carbon[10] (*sensu* Ferrari and Robertson[10]) and coal[11], all of which are thermally altered organic matter, would have well developed disordered band (D band) at ~1350 (cm^{-1}) and graphite band (G band) at ~1580 (cm^{-1})[10,11]. The D band is attributable to structural defects and heteroatoms whereas the G band is usually contributed by the in-plane vibration of carbons in graphene sheets with E_{2g2} symmetry[11]. The spectral position of D and G bands are very similar to the 1349, 1565, and 1607 (cm^{-1}) mentioned by Norell et al.[3].

The Raman spectra of 'soft *Mussaurus* eggshell' in the spectral region of 1000–1650 (cm^{-1}) is remarkably similar to Raman spectra reported from fully-calcified archosaur eggshells from the Upper Cretaceous of South Korea[5,12] (Fig. 1a,b,d–f) that were inferred to have experienced 200–300 °C during their taphonomic history and other thermally altered organic matter that have reached around 250–300 °C in their burial history[11]. This is unsurprising considering the fact that the fossil locality of *Mussaurus* eggs (Laguna Colorada Formation) was deposited in a post-rift thermally induced basin[13]. Therefore, the interpretation of two broad bands in 1000–1650 (cm^{-1}) of *Mussaurus* eggshell as a sign of PFPs (*N*-, *S*-, *O*-heterocyclic polymers) is doubtful based on the works of organic (geo)chemists[9–11]. The assignment of the peaks of 1349, 1565, and 1607 (cm^{-1}) to PFPs[3] would be convincing only after excluding the possibility of D and G bands of amorphous carbon[5,9–12].

Thirdly, the absence of birefringence in *Mussaurus* eggshell may not be completely indicative of an absence of biogenic calcite. Norell et al.[3] reported that *Mussaurus* eggshell lacks birefringence and thus claimed the absence of calcite. However, such an absence of birefringence could be a result of the excessive thickness of the thin section. Norell et al.[3] indicated that the *Protoceratops* egg thin section was made to 30-μm-thick, yet the thickness of the thin section of *Mussaurus* egg was not reported. In addition, in a 12-μm-thick thin section of fully-calcified, rigid passerine eggshell, the high amount of organic matters in the squamatic zone hinders the calcite birefringence, which is significantly different from the mammillary layer with a less amount of organic matters and clear birefringence (Fig. 1g; see also Fig. 1h). It thus suggests that an absence (or at least weakness) of birefringence in *Mussaurus* eggshell may be attributable to other reasons such as amorphous carbon[5,12] or calcite grain size[14] instead of the absence of calcite. Moreover, a distinctive cone-shaped shell unit with faint curved accretion outline appears at inner surface of the *Mussaurus* eggshell (Norell et al.[3], fig. 1e, bottom left), although the thin section appears to be too thick to show the detailed microstructure. A more adequately prepared thin section in combination with an observation under scanning electron microscope (SEM) are required for revealing the detailed micro- and ultra-structure of the *Mussaurus* eggshell.

In summary, there are methodological flaws in Norell et al.[3], especially in the interpretation of *Mussaurus* eggshell, and it may influence the conclusion of study. Correctly addressing the mechanical properties of *Mussaurus* eggshell is fundamental in discussion of the ancestral condition of dinosaur eggshell. We tentatively changed the character state of *Mussaurus* eggshell into ‘rigid’ and reran the dataset of Norell et al.[3]. The results show that the ancestral state of the eggshell mechanical property of the first dinosaur changes from soft (92% likelihood proportion in the Norell et al.[3]) to probably rigid with somewhat equivocal likelihood (52% likelihood proportion) (Fig. 2). The working hypothesis of Norell et al.[3] (see also Stein et al.[15]), although exciting, needs to be supported by additional analysis and maybe additional specimens.

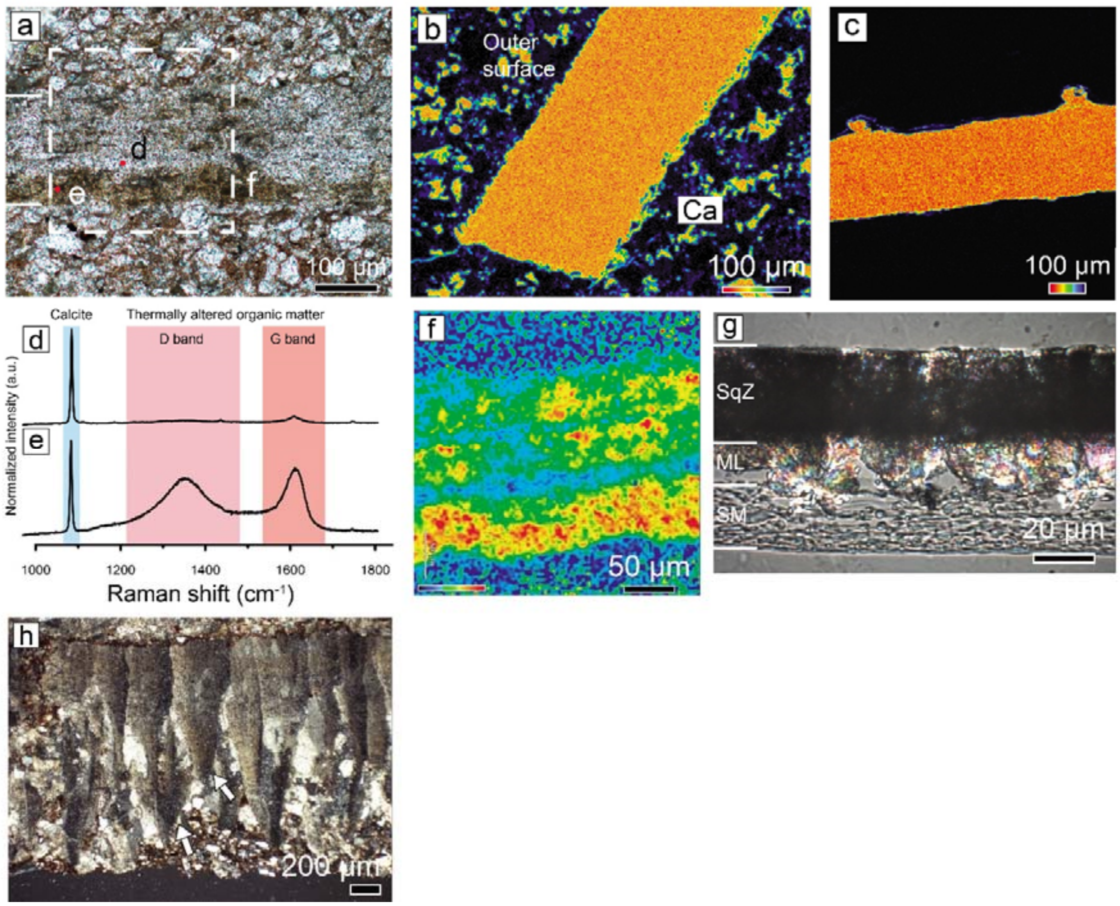

Fig. 1 Analytical data from modern and fossil eggshells. a,b, *Aenigmaoolithus vesicularis*, an eggshell type from the Wido Volcanics of South Korea. A thin section image of eggshell bounded by two white bars (a). Raman spectra were acquired from two red dots and mapping from a dashed square. Distribution of Ca in the eggshell and surrounding sediments detected by EPMA (b). Note that the rigid calcified eggshell is completely composed of calcite while sedimentary calcite shows patchy distribution, which we expect from the *Mussaurus* eggshell. The red part in the scale bar corresponds to a higher amount of Ca. Modified from Choi et al.[5]. **c**, Rigid eggshell of *Gekko gecko* (Squamata) shows similar Ca distribution with that of *A. vesicularis*. Modified from Choi et al.[14]. **d,e**, The Raman spectrum targeted at the transparent part of *A. vesicularis* only shows the presence of calcite (d) while the Raman spectrum at the dark part (e) shows clear signals of calcite, D and G bands. Modified from

Choi et al.[5]. **f**, A Raman mapping showing the distribution of amorphous carbon detected by G band position (~1580 cm^{-1}). The distribution of amorphous carbon (f) is consistent with dark part of the eggshell section (a). Modified from Choi et al.[5]. **g**, A 12-μm-thick thin section image of *Serinus canaria* (passerine) eggshell. Note that the birefringence is not clear in the squamatic zone despite the presence of calcite. ML, mammillary layer; SM, shell membrane; SqZ, squamatic zone. **h**, A 50-μm-thick thin section image of *Dendroolithus wangdianensis* (dinosaur eggshell). Note that birefringence is not observed in the area marked by white arrows despite the presence of calcite.

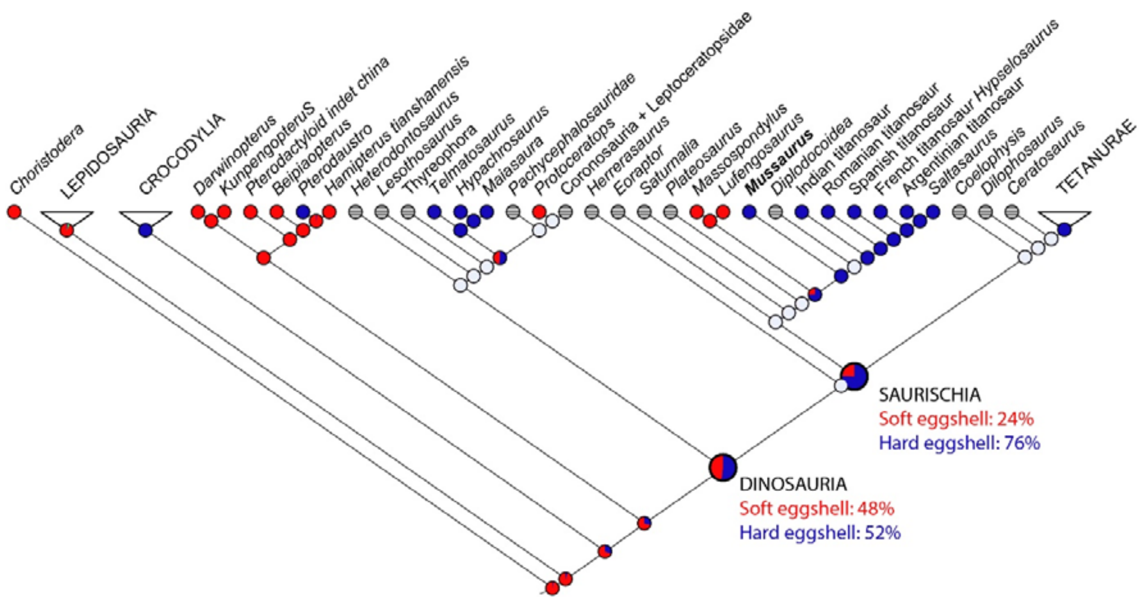

Fig. 2 Likelihood based ancestral character reconstruction for eggshell mechanical properties in Diapsida. The methodology used to obtain this reconstruction is identical to the one used by Norell et al.[3], but with *Mussaurus* state coded as '2', rigid-shelled. Red, soft eggshell; blue, rigid eggshell; grey stripes, unknown character state.

Data availability

No new data were generated in this study.

1. Norell, M. A. et al. A theropod dinosaur embryo and the affinities of the Flaming Cliffs dinosaur eggs. *Science* **266**, 779–782 (1994).

2. Chiappe, L. M. et al. Sauropod dinosaur embryos from the Late Cretaceous of Patagonia. *Nature* **396**, 258–261 (1998).

3. Norell, M. A. et al. The first dinosaur egg was soft. *Nature* **583**, 406–410 (2020).

4. Moreno-Azanza, M., Mariani, E., Bauluz, B. & Canudo, J. I. Growth mechanisms in dinosaur eggshells: an insight from electron backscatter diffraction. *J. Vertebr. Paleontol.* **33**, 121–130 (2013).

5. Choi, S., Lee, S. K., Kim, N.-H., Kim, S. & Lee, Y.-N. Raman spectroscopy detects amorphous carbon in an enigmatic egg from the Upper Cretaceous Wido Volcanics of South Korea. *Front. Earth Sci.* **7**, 349 (2020).

6. Yang, T.-R., Chen, Y.-H., Wiemann, J., Spiering, B. & Sander, P. M. Fossil eggshell cuticle elucidates dinosaur nesting ecology. *PeerJ* **6**, e5144 (2018).

7. Moreno-Azanza, M., Bauluz, B., Canudo, J. I., Gasca, J. M. & Torcida Fernández-Baldor, F. Combined use of electron and light microscopy techniques reveals false secondary shell units in Megaloolithidae eggshells. *PLoS ONE* **11**, e0153026 (2016).

8. Wiemann, J. et al. Fossilization transforms vertebrate hard tissue proteins into N-heterocyclic polymers. *Nat. Commun.* **9**, 4741 (2018).

9. Sadezky, A., Muckenhuber, H., Grothe, H., Niessner, R. & Pöschl, U. Raman microspectroscopy of soot and related carbonaceous materials: Spectral analysis and structural information. *Carbon* **43**, 1731–1742 (2005).

10. Ferrari, A. C. & Robertson, J. Interpretation of Raman spectra of disordered and amorphous carbon. *Phys. Rev. B* **61**, 14095–14107 (2000).

11. Henry, D. G., Jarvis, I., Gillmore, G. & Stephenson, M. Raman spectroscopy as a tool to determine the thermal maturity of organic matter: application to sedimentary, metamorphic and structural geology. *Earth-Sci. Rev.* **198**, 102936 (2019).

12. Choi, S. et al. Fossil eggshells of amniotes as a paleothermometry tool. *Palaeogeogr. Palaeoclimatol. Palaeoecol*. **571**, 110376 (2021).

13. Pol, D. et al. Earliest evidence of herd-living and age segregation amongst dinosaurs. *Sci. Rep.* **11**, 20023 (2021).

14. Choi, S., Han, S., Kim, N.-H. & Lee, Y.-N. A comparative study of eggshells of Gekkota with morphological, chemical compositional and crystallographic approaches and its evolutionary implications. *PLoS ONE* **13**, e0199496 (2018).

15. Stein, K. et al. Structure and evolutionary implications of the earliest (Sinemurian, Early Jurassic) dinosaur eggs and eggshells. *Sci. Rep.* **9**, 4424 (2019).

Acknowledgements We thank Jingbo Nan (Southern University of Science and Technology, China) for discussion and anonymous referees who greatly improved the manuscript. S.C. was supported by Basic

Science Research Program through the National Research Foundation of Korea funded by the Ministry of Education (grant number: 2020R1A6A3A03038316); T.-R.Y. was supported by the research funding from the Ministry of Science and Technology, Taiwan (MOST 108-2116-M-178-003-MY2); M.M.A. was supported by Fundação para a Ciência e a Tecnologia (PTDC/CTA-PAL/31656/2017 and SFRH/BPD/113130/2015) and the Spanish Ministry of Science and Innovation (project CGL2017-85038-P) and by the Government of Aragón-FEDER 2014–2020.

Author contributions All authors conceived, wrote, and edited the manuscript.

Competing interests The authors declare no competing interests.

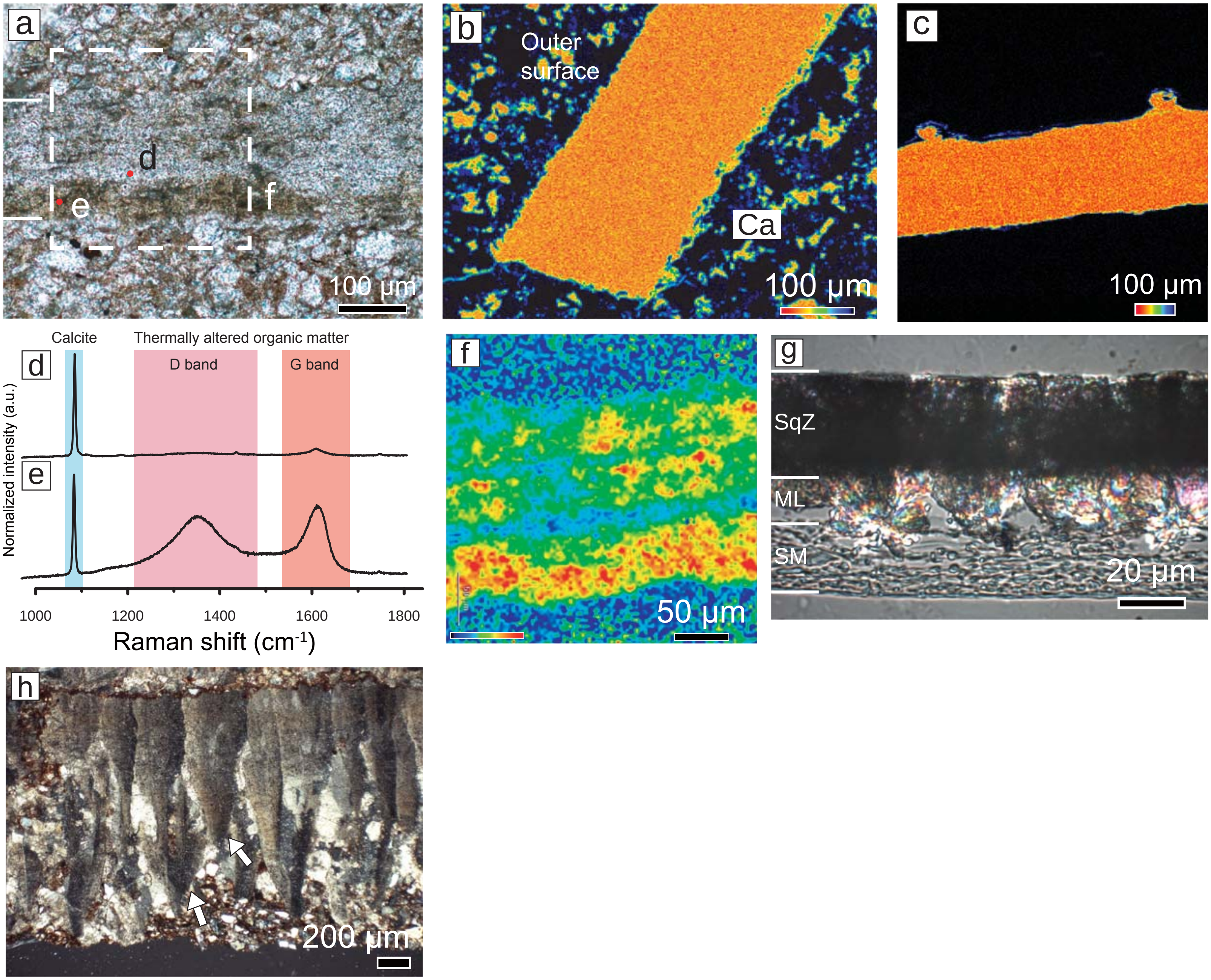

a
d
e
f
100 µm
b
Outer surface
Ca
100 µm
c
100 µm
Calcite
Thermally altered organic matter
D band
G band
d
e
Normalized intensity (a.u.)
1000
1200
1400
1600
1800
Raman shift (cm-1)
f
50 µm
g
SqZ
ML
SM
20 µm
h
200 µm

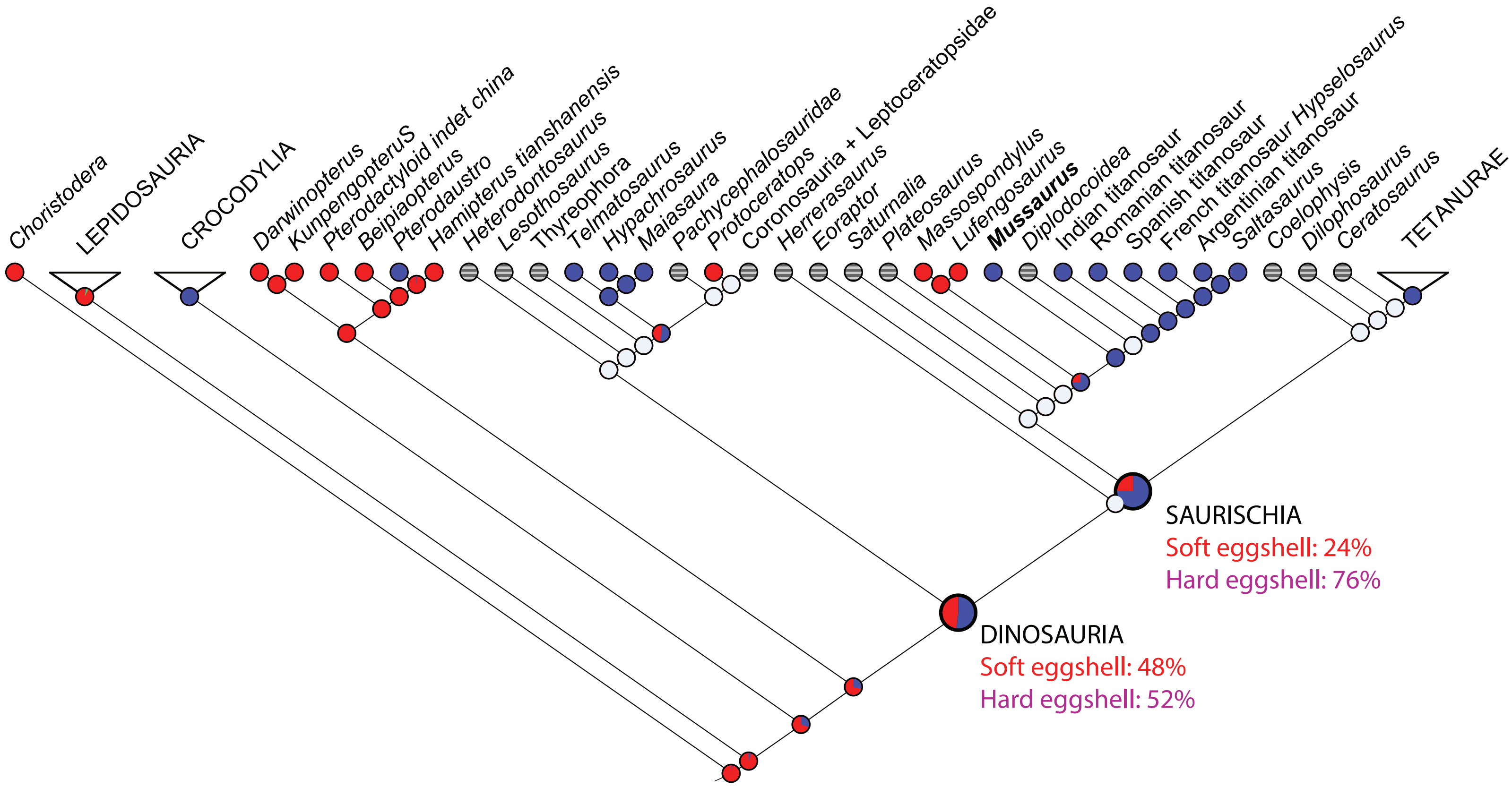

Choristodera
LEPIDOSAURIA
CROCODYLIA
Darwinopterus
KunpengopteruS
Pterodactyloid indet china
Beipiaopterus
Pterodaustro
Hamipterus tianshanensis
Heterodontosaurus
Lesothosaurus
Thyreophora
Telmatosaurus
Hypachrosaurus
Maiasaura
Pachycephalosauridae
Protoceratops
Coronosauria + Leptoceratopsidae
Herrerasaurus
Eoraptor
Saturnalia
Plateosaurus
Massospondylus
Lufengosaurus
Mussaurus
Diplodocoidea
Indian titanosaur
Romanian titanosaur
Spanish titanosaur
French titanosaur Hypselosaurus
Argentinian titanosaur
Saltasaurus
Coelophysis
Dilophosaurus
Ceratosaurus
TETANURAE
SAURISCHIA
Soft eggshell: 24%
Hard eggshell: 76%
DINOSAURIA
Soft eggshell: 48%
Hard eggshell: 52%